2014 IEEE International Conference on Robotics & Automation (ICRA)
Hong Kong Convention and Exhibition Center
May 31 - June 7, 2014. Hong Kong, China

Grid-based Mapping and Tracking in Dynamic Environments using a Uniform Evidential Environment Representation

Georg Tanzmeister, Julian Thomas, Dirk Wollherr and Martin Buss

Abstract— **Mapping and tracking in dynamic environments for autonomously-moving robots is still challenging, despite being essential tasks. They are often done separately using occupancy grids and established object tracking algorithms. In this work, an approach is presented that estimates a uniform, low-level, grid-based world model including dynamic and static objects, their uncertainties, as well as their velocities. It does not require existing object tracks to filter out data points not used for creating and updating the map. Nor does it require that measurements can be classified into belonging to a static or to a moving object. Promising results from experiments with an autonomous vehicle equipped with a laser scanner demonstrate the usefulness of the approach.**

I. Introduction

Mapping and tracking are typically done as separate tasks. While for the former, feature-less occupancy grid mapping [1] is well established, the latter is often done using model and shape assumptions. In occupancy grid mapping, the world is assumed to be static and thus the occupancy probability of each cell represents the probability of that cell being occupied by a static object. The environment is, however, rarely entirely static. If measurements from dynamic objects are integrated into the grid, artifacts occur. This can lead to problems in navigation, consider, e.g., an autonomous vehicle driving behind another vehicle.

If a sensor is used that cannot measure the dynamics of a point in space, e.g., a laser scanner, often inconsistencies between the map built so far and the current scan are used to detect and filter out those measurements [2]–[6]. Sometimes, the Dempster-Shafer theory of evidence is used to better model these inconsistencies as conflicts [7]. Using inconsistencies as evidence for dynamic information, however, conflicts the original idea of filtering sensor measurements to incorporate for noise. In addition, such approaches often fail, e.g., at objects moving perpendicular to the sensor.

As important as a robust representation of the static environment, is the representation of the dynamic environment. In some work, the inconsistencies during mapping are used as input to an object tracker [4]–[6] and most notably SLAM and DATMO [4]. In other work, it is directly relied on an object tracker [8] to filter out the corresponding measurements that are then not used to update the stationary grid. Obviously though, relying on object tracking simply transfers the problem and with the notion of objects and tracks, in comparison to cells or data points, comes the data association problem. All of the above approaches have in common that the decision of whether a single sensor measurement is used to update the grid, is binary and its uncertainty is not modeled. In addition, separating mapping and tracking leads to inconsistencies between the representations.

There are also approaches that combine the estimation of the static and the dynamic environment. In [9] Rao-Blackwellized SLAM is combined with conditional particle filters for tracking, but measurements need to undergo classification into static or dynamic. In SLAMMOT [4] a joint posterior over all generalized objects and the robot pose is calculated. It is, however, in general computational infeasible as the authors point out, and builds upon the notion of objects requiring features and data association. A model-free, grid-based approach is the Bayesian Occupancy Filter (BOF) [10]. It uses a four-dimensional grid, i.e. two dimensions for the location plus two dimensions for the velocity. Apart from scaling and computational issues regarding 4-D grids, the velocities need to be discretized. Extensions were made to work in two dimensions [11], while still requiring velocity discretization, and to increase performance by using an existing map of the environment [12], [13].

In a different, particle-based approach [14] the velocities do not need to be discretized but are estimated as continuous distribution. The particles have a position and speed and can move freely between cells. The authors describe the particles as both, velocity hypotheses and the building blocks of the environment. The particles in a particular cell represent, on the one hand, the velocity distribution and on the other does the number of particles represent the occupancy likelihood. The exact role of the particles and the probability distribution that is approximated stays, however, unclear. In addition, the resulting grids do not model free-space and seem noisy. We still find the idea very promising and use it as base for part of our work.

In this work, a novel evidential framework for simultaneously mapping and tracking of the environment is presented. It uses a uniform, grid-based representation without the need of shape assumptions nor data association. It also does not require measurements to be pre-classified into static or dynamic and is able to model their uncertainty. The rest of the paper is structured as follows. In Section II we build upon the work from [14] and formulate a particle filter-based dynamic environment estimator. In Section III, the evidential framework is introduced, which robustly represents the static world, the free space and the dynamic world. And finally, in Section IV experimental results are given.

G. Tanzmeister and J. Thomas are with BMW Group Research and Technology, D-80992 Munich, Germany, {georg.tanzmeister, julian.thomas}@bmw.de.

D. Wollherr and M. Buss are with the Institute of Automatic Control Engineering of the Technische Universität München, D-80290 Munich, Germany, {dw, mb}@tum.de.

978-1-4799-3684-7/14/$31.00 ©2014 IEEE

II. Grid-based Estimation and Tracking of the Dynamic Environment using Particle Filters

In this section, the particle filter-based dynamic estimator is given. The approach works on the cell level and thus without object shape assumptions. As described above, it is built upon the ideas presented in [14], but this paper presents a different formulation. In addition, it is shown how continuous evidences for static and dynamic can be deduced, which will be used in Section III.

A. Overview

The goal of the method given in this section is to estimate a map v_t of velocity distributions at a particular time instance t. Every cell i of the velocity map $v_t = \{v_t^i\}$ has attached to it a random vector $V = (V_x,\ V_y)^T$ that represents the velocity distribution in the x and y direction. The cells, however, although representing dynamic information, are a fixed discretization of the world in individual areas that do not move in space.

Similar to occupancy grid mapping, the problem of estimating the map posterior $p(v_t|z_{1:t}, x_{1:t})$ given the measurements $z_{1:t}$ and the robot poses $x_{1:t}$ is broken down into estimating $p(v_t^i|z_{1:t}, x_{1:t})$ for every cell i using the assumption that the cells are independent in a single time instance t

$$p(v_t|z_{1:t}, x_{1:t}) = \prod_i p(v_t^i|z_{1:t}, x_{1:t}). \tag{1}$$

Notice that the cells are only independent within t. This does not hold over consecutive time instances, as dynamic objects move over cells over time. In other words, it is assumed that the velocity distribution v_t^i of cell i is independent of v_t^j of cell j at time t. This assumption is, arguably, as strong as the cell occupancy independence in the standard occupancy grid mapping algorithm. From time instance $t-1$ to t, however, the full map posterior is used for the calculation $p(v_t^i|z_{1:t}, x_{1:t})$ of a particular cell i

$$p(v_t^i|z_{1:t}, x_{1:t}) = \int p(v_t^i|v_{t-1}, z_{1:t}, x_{1:t}) p(v_{t-1}|z_{1:t-1}, x_{1:t-1})\, \mathrm{d}v_{t-1}. \tag{2}$$

B. Estimating Cell Velocities using Particle Filters

Particle Filters, as described e.g., in [15], are a nonparametric and often used version of the Bayes filter. They have proven to be very efficient for low-dimensional problems, such as localization and also for solving the SLAM problem, e.g. FastSLAM, where Rao-Blackwellization is used to factorize the full posterior into a localization term, implemented using particles, and a mapping term, where the robot pose is assumed to be known [16].

In this approach, the independence assumption from (1), is used so that particles can represent low-dimensional velocity hypotheses, rather than full maps. The particles are at a continuous position in the grid, on creation at the cell center, and represent velocity and orientation hypothesis, or more precisely a particular $v_x,\ v_y$. They move according to their motion vector and a certain motion model between time steps and are not fixed to their original cell in which they have been created. Although the particles move through the grid, at a particular time instance t, every particle belongs to a particular cell i and is thus one particular sample of the motion distribution of that cell. In other words, every cell carries its own particle filter. The particles, however, can move between the cells and thus between the particle filters. The map posterior

$$p(v_t|z_{1:t}, x_{1:t}) = \prod_i p(v_t^i|z_{1:t}, x_{1:t}) \tag{3}$$

$$= \prod_i \sum_{v^i_{t,[k]}} w_{[k]} \delta_{v^i_{t,[k]}}(v_t^i) \tag{4}$$

can thus be seen as product of velocity distributions represented by a sum of weighted particles, where $\delta_{v_t^i}$ represents the Dirac delta function at v_t^i.

C. Particle Sampling

Sampling is an essential part of every particle filter. Typically, as in Monte-Carlo localization, the initial distribution is uniform. It is updated in every step through a weighted resampling procedure, which is then used to calculate the sampling distribution of the next time step, e.g., by applying a motion model on each particle. In general, the concept is very similar here. Formally, particle k is sampled from

$$v^i_{t,[k]} \sim p(v_t^i|v_{t-1}). \tag{5}$$

Applying uniform initial sampling as in [14], makes it however impossible to exactly represent static objects, since $P(V = (0,0)^T) = 0$. It is therefore proposed to add a Dirac delta impulse δ_0 centered at $(v_x, v_y)^T = (0,0)^T$ to the uniform distribution $\mathcal{U}$

$$p(v^i) = w_1 \mathcal{U}_{\pm v_{\max}}(v^i) + w_2 \delta_0(v^i) \tag{6}$$

in order to better represent the world. The two weights w_1, w_2 represent the priors of the amount of dynamic and static information respectively.

It is clear that, if, for every cell, of which there are l^2 for a grid of width and height l, n particles are created, the number of particles explodes if the grid size increases. Fortunately though, most of the cells are either free space or space that cannot be observed and only occupied cells can be used to derive reasonable velocities. Particles are, however, also allowed to exist in the other areas to compensate for missed detections and occlusions and the weighted resampling, described in the next section, assures that the number of particles still stays approximately constant over time, depending on the number of occupied grid cells.

D. Particle Weighting and Resampling

In a particle filter, the weight of each particle represents how well that particular sample fits the data and is calculated by dividing the target distribution, the one that ought to be estimated, by the proposal distribution, the one where samples are generated from. Dividing the target

$$p_{\text{target}} = p(v_{1:t}|z_{1:t}, x_{1:t}) \tag{7}$$

by the proposal distribution

$$p_{\text{proposal}} = p(v_{1:t}|z_{1:t-1}, x_{1:t}) \tag{8}$$
$$= p(v_t|v_{t-1}, x_t)p(v_{1:t-1}|z_{1:t-1}, x_{1:t-1}) \tag{9}$$

yields, unsurprisingly,

$$\frac{p_{\text{target}}}{p_{\text{proposal}}} = \frac{p(v_{1:t}|z_{1:t}, x_{1:t})}{p(v_t|v_{t-1}, x_t)p(v_{1:t-1}|z_{1:t-1}, x_{1:t-1})} \tag{10}$$
$$= \eta p(z_t|v_t, x_t) \tag{11}$$

the measurement model and, assuming independence, the weight $w_{[k]}$ of particle $v^i_{t,[k]}$ yields

$$w_{[k]} = \eta p(z^i_t|v^i_{t,[k]}, x_t). \tag{12}$$

Velocities can, however, rarely be measured directly, such as with a laser scanner, which is also the sensor used in this work. Thus it cannot be decided whether or not a particular sample within one time frame t and within one cell fits the data better than any other sample in the same cell at t. Since the particles are not fixed to one and the same cell over individual time steps, they can still be weighted on a cell level. Intuitively, a particle that moves through the grid, fits the real world dynamics well, if every cell on its path was receiving sensor data at the time that particle was in that particular cell.

In this work, likelihood fields [15] are used as observation model. The minimum probability, though,

$$\min_i(p(z^i_t|v^i_{t,[k]}, x_t)) = p_{\text{survival}} \tag{13}$$

is the probability that a particle survives, even if that cell or any cell in the neighborhood is not observed. As in the standard particle filter algorithm, the weight, which is equal for all particles in a cell, describes how likely it is that a particle survives.

E. From Velocity Probability Distributions to Dynamic and Static Evidences

So far, the velocity grid estimator is presented. For every cell in the grid a velocity probability distribution is calculated using particle filters. Those velocity probability distributions are a useful information and can be seen as a cell-based tracking algorithm. In order to compute static occupancy grids as well as maps that only contain the dynamic part of the environment, a classification between static and dynamic based on the velocity distribution is needed. In [14] a classifier based on the mean and the variance is used. If the absolute values of all components of the velocity mean are lower than twice their standard deviation, the cell is static, otherwise it is dynamic. The idea of the classification from [14] is that static cells can be seen roughly as those, where the velocity distribution, starting with a uniform distribution, has not converged yet to a Gaussian distribution that represents the estimated velocity of the underlying moving object. Hence, the static parts are detected indirectly, as where the particle filters fail to converge to a peak distribution or where the mean velocity is low. Drawbacks of this approach are, that at static obstacles the particles will leave the cells of the object and new particles have to be continuously created. The classification also correlates with the motion noise applied in the motion update, since if it is too low, the variance will be too low and there is a strong bias towards the class dynamic. Nevertheless, for dynamic evidences, the idea that a good track of a moving object shows a peak distribution, under the assumption that a cell is completely covered by only one object, is adopted in a modified way as a weighting factor, as shown below.

Since in this work, the particles are drawn from a different distribution and pure static particles, i.e. where $v_x = v_y = 0$, are used, see Section II-C, static and dynamic particles can directly be detected based on their velocity. Another difference is, that this paper does not aim for a binary decision but infers continuous evidences. This approach uses the Dempster-Shafer theory of evidence, as will be shown in the next section, to compute the aforementioned uniform environment model and thus belief masses are deduced.

Let $X = X_S \cup X_D$ be the set of all particles of a particular cell that have survived at least t steps, in order to incorporate the fact that velocities are estimated indirectly over multiple time instances. $X_S = \{v_{[k]} \mid v_{[k]} \in X \wedge ||v_{[k]}|| \leq \varepsilon\}$ and $X_D = \{v_{[k]} \mid v_{[k]} \in X \wedge ||v_{[k]}|| > \varepsilon\}$ hold the static and the dynamic particles, respectively. The parameter ε is used instead of 0 to discard particles that move very slowly through the cells belonging to a static object. The evidential belief masses for static, dynamic and unknown

$$m(S) = \frac{|X_S|}{n} \tag{14}$$
$$m(D) = \left(1 - \frac{|\sigma|}{\sigma_{\max}}\right)\frac{|X_D|}{n} \tag{15}$$
$$m(\Theta) = 1 - m(S) - m(D) \tag{16}$$

are calculated based on their set cardinality, where σ is the standard deviation of the orientation of all $v_{[k]} \in X_D$. Fig. 1 shows a comparison between the approach of [14] and the one of this paper. To exclude the effects of noise, the same scan grid from real laser data is used as input for every time step. In addition a moving object exhibiting constant velocity is simulated to show evidences for both, static and dynamic. Although the approach of [14] shows slight convergence behavior, since at static objects, fast moving particles die out, it never converges to a stable correct result. Even for a large number of iterations, the result looks similar to the bottom row of Fig. 1b. Note in comparison the convergence property of this approach as well as the continuous measure. Next, it will be shown how the belief masses are used to create a unifying environment model.

III. Evidential Grid Mapping in Dynamic Environments

Having a cell-based estimator for the dynamics, it is now possible to represent a unifying grid-based model of the environment. Although the particle map from the previous section already estimates static and dynamic evidences, they do not directly correspond to filtered occupancy probabilities.

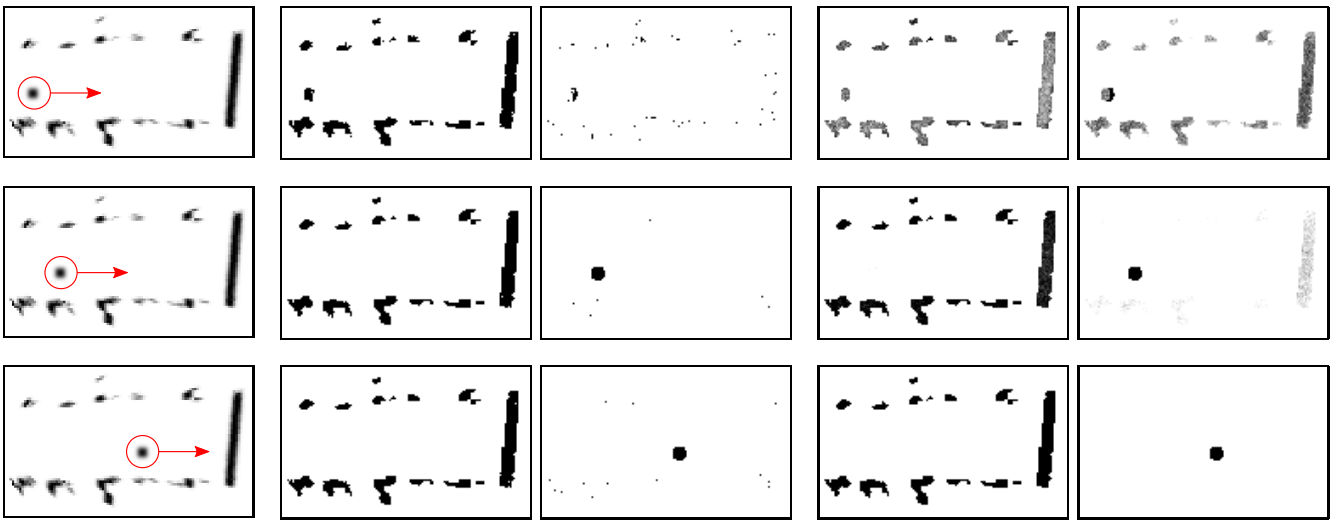

(a) Scan grid.

(b) Approach of [14], static (left) and dynamic (right) classifications.

(c) This paper, static (left) and dynamic (right) belief masses. Static and dynamic particles are equally likely.

Fig. 1. Comparison between the approach of [14] and this paper. Top row depicts the result at $t = 2$, middle row at $t = 10$ and bottom row at $t = 30$. Particles that have survived at least 2 time steps are accounted for classification. Note the convergence property.

The particle map may contain noise, since, whenever the scan grid measures a previously unoccupied cell, particles are created, initially at random, in order to estimate the velocities of dynamic objects. In addition, free-space as well as yet unobserved areas are not modeled in the particle world. Contrary to the work in [14], where occupancy probability was chosen to correspond to the number of particles, evidences for static occupancy as well as for free space are calculated by filtering the beliefs over time.

A. Environment Model

Similar to other work [7], [17], [18], the Dempster-Shafer theory of evidence is used for computing the uniform environment representation m_t at time t. This paper, though, proposes to use a different frame of discernment than the commonly used free-occupied model. In this work, the frame of discernment

$$\Theta = \{F, S, D\} \tag{17}$$

represents hypotheses for free space, for static occupancy and for dynamic occupancy. In the Dempster-Shafer theory of evidence, every element of the power set of the frame of discernment 2^Θ is considered. Practically, in this work, only the elements $\{\ \emptyset,\ \{F\},\ \{S\},\ \{D\},\ \{S,\ D\},\ \Theta\ \}$ are used, since $\{F,\ S\}$ and $\{F,\ D\}$ are always zero.

To the best of our knowledge, an $\{F, S, D\}$ model for grid mapping has not been used before. This model allows for a direct integration of static and dynamic information into $\{S\}$ and $\{D\}$ respectively, as well as of sensor data, e.g., from a laser scanner, where no distinction between static and dynamic is possible, by using $\{S,\ D\}$.

B. Single-Frame Information Fusion

As described above, the particle map from the previous section calculates cell velocities of the environment and deduces belief masses for $\{S\}$ and $\{D\}$. Free space, however, as well as robustness over noise is not yet represented. To overcome this, the static and dynamic evidences are fused with free space information and filtered over time.

Free space information comes from an inverse beam sensor model [19] similar to what is used in standard occupancy grid mapping, but instead of occupancy probabilities, evidences for $\{F\}$ and $\{S,\ D\}$ are deduced. Although the raw data for the inverse sensor model comes from the same sensor as the input data for the particle map, the basic belief assignments have different focal elements, i.e. they carry non-zero belief masses for different subsets of 2^Θ. The particle map and the inverse sensor model can be seen like different sensors measuring different, partially-complementary information that is fused to extract a complete representation of the environment.

The fusion of the belief of the inverse sensor model, denoted by s_1, and of the particle map, denoted by s_2, is done using the non-normalized Dempster's rule of combination, also known as conjunctive rule

$$m_s(A) = (m_{s_1} \oplus m_{s_2})(A) = \sum_{B \cap C = A} m_{s_1}(B) m_{s_2}(C) \tag{18}$$

$\forall A \subseteq \Theta \neq \emptyset$ and the conflict

$$K = \sum_{B \cap C = \emptyset} m_{s_1}(B) m_{s_2}(C) \tag{19}$$

is not resolved by normalization, like in Dempster's rule but resolved explicitly. In this work, the conflict

$$K = m_{s_1}(F) m_{s_2}(S) + m_{s_1}(F) m_{s_2}(D) \tag{20}$$

may only arise between free-static and free-dynamic. Empirically, it is chosen to transfer K to $m_s(F)$, since the inverse sensor model evidences are closer to the raw sensor data. Note that the cell index i is dropped.

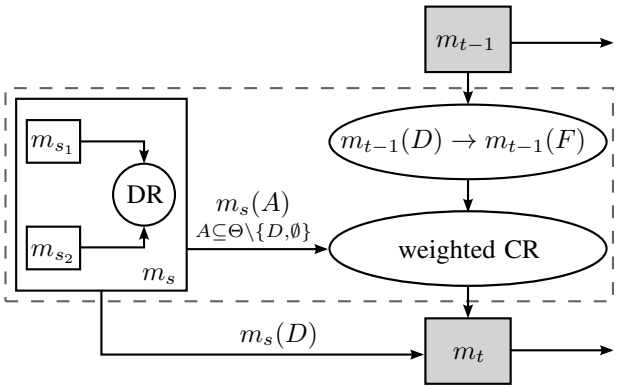

Fig. 2. Overview of belief fusion using Dempster's combination rule (DR) and a weighted variant of Jøsang's cumulative rule (CR).

C. Filtering

In contrast to the previous section, where different focal elements are fused to yield a logical combination, it was shown that Dempster's rule is not the correct operator for cumulative belief fusion, but only represents an approximation in such situations [20]. Therefore, in this work, Jøsang's cumulative operator [20] is used for temporal filtering.

The rule is, however, not applied to the belief mass of D. The belief of dynamic is deduced from the estimated velocity distributions in the particle map through the movement of the particles. Filtering the dynamic evidences would require moving the evidences from the previous step according to the velocity distribution, which is already done in the particle map. In addition, the filtering would not react quickly enough to detect new moving objects as well as to allow a moving object driving over free space. Therefore, the fused belief mass $m_t(D)$ is used directly from the particle map.

First, the dynamic mass of m_{t-1} is moved to free

$$m_{t-1}(F) = m_{t-1}(F) + m_{t-1}(D) \tag{21}$$
$$m_{t-1}(D) = 0. \tag{22}$$

Then, a weighted version of Jøsang's cumulative operator

$$m_t(D) = m_s(D) \tag{23}$$

$$m_t(A)_{A \subset \Theta \setminus \{D,\emptyset\}} = w \frac{m_{t-1}(A)m_s(\Theta) + m_{t-1}(\Theta)m_s(A)}{m_{t-1}(\Theta) + m_s(\Theta) - m_{t-1}(\Theta)m_s(\Theta)} \tag{24}$$

$$m_t(\Theta) = w \frac{m_{t-1}(\Theta)m_s(\Theta)}{m_{t-1}(\Theta) + m_s(\Theta) - m_{t-1}(\Theta)m_s(\Theta)} \tag{25}$$

with the normalization weight

$$w = \frac{(1 - m_s(D))(m_{t-1}(\Theta) + m_s(\Theta) - m_{t-1}(\Theta)m_s(\Theta))}{\sum_{A \subset \Theta \setminus \{D,\emptyset\}} m_{t-1}(A)m_s(\Theta) + m_{t-1}(\Theta)m_s(A)} \tag{26}$$

is applied to all but the dynamic mass, which is directly used from the fused scan. In Fig. 2 an overview of the update rule is shown.

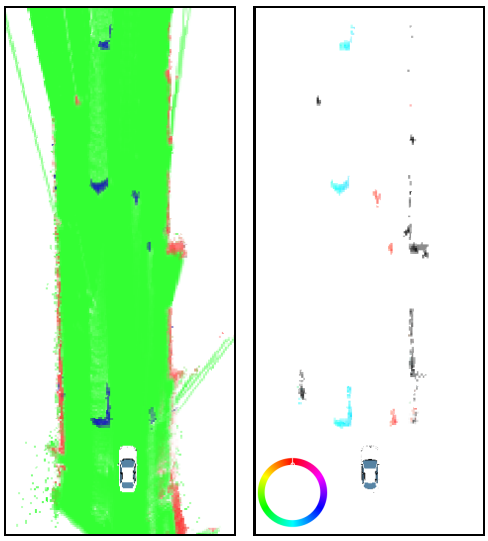

(a) Resulting uniform world representation. (b) Velocity map.

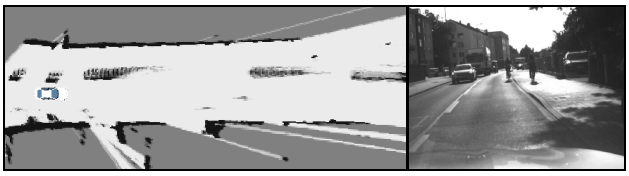

(c) Standard occupancy grid. (d) Camera image.

Fig. 3. Urban scene showing 3 bicycles and 3 vehicles. Robot is moving.

IV. Results

The algorithm was tested qualitatively on real data coming from a vehicle equipped with a 4-layer laser scanner, which is mounted under the front number plate, driving in an urban environment. The grid resolution was set to 512×512 and the cell size was $0.2\,\text{m}$. The velocity range in the particle map was set to $\pm 70\,\text{km/h}$, the probability of sampling a static particle was 0.3 and the particle survival probability was 0.5. The maximum number of particles per cell was set to 50.

Two scenes are shown. The first, depicted in Fig. 3, shows the successful detection and tracking of 3 bicyclists, riding in the same direction as the robot, as well as 3 vehicles coming towards it. Fig. 3a shows the resulting world representation. Green, Red and Blue represent the free space, the static cells and the dynamic cells respectively. The colors are mixed via alpha compositing, where the alpha value represents the evidential mass. Unknown is shown as white. Fig. 3b shows the velocity map using an HSV color coding, where the hue represents the direction, as given in the image, the saturation the dynamic evidence and the value $1 - m_t(S)$. Also shown are a standard occupancy grid for comparison and the camera image. The second scene, given in Fig. 4, shows a traffic crossing exhibiting multiple objects and a high amount of occlusion. Note especially the artifacts from the dynamic objects in the standard occupancy grid map, making reasoning and navigating difficult. Note also, that no assumptions about the environment are made and that the representation is low-level. No objects exist and thus any

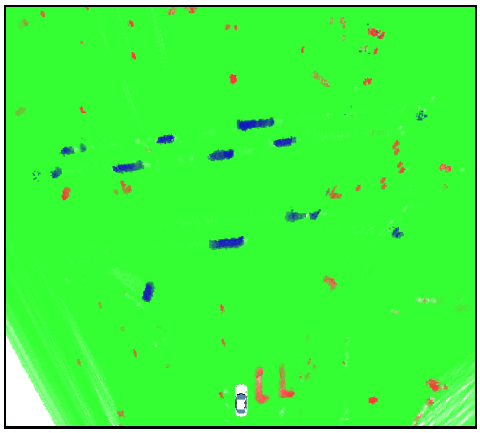

(a) Resulting uniform world representation.

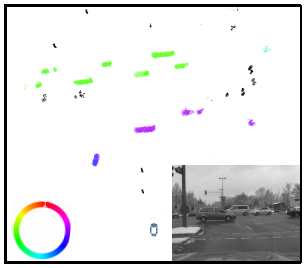

(b) Velocity map and camera image.

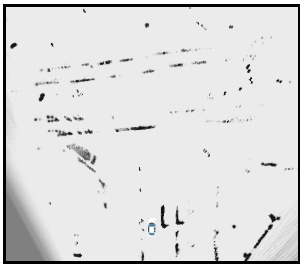

(c) Standard occupancy grid.

Fig. 4. Road junction with a high amount of traffic and occlusion demonstrating the performance of the uniform environment model. Robot has stopped at traffic light.

shape can be represented and no data association is needed. The environment model presented in this paper, represents free space, dynamic cells, static cells and occupied cells, i.e. static-dynamic cells, where the distinction between static and dynamic has not been made yet, all as continuous evidences in the Dempster-Shafer framework. A video demonstrating the results is attached with this contribution. Despite the good results in the given scenarios, there are also scenes where the approach has difficulties. Especially continuous, elongated, static structures such as guard rails, where the sensor has difficulties in capturing it, are likely to be misclassified as dynamic cells moving beside the robot at the same speed.

V. Conclusion and Future Work

The paper presents an approach for estimating a map and for tracking the environment in a uniform grid-based model. It allows the integration of uncertainty of whether sensor measurements belong to static or to dynamic objects in a novel evidential framework. In this model tracks and objects do not exist and therefore the data association problem is not present. In addition, no feature extraction or shape assumptions about the moving objects are needed and thus arbitrary objects can be tracked. The utility of the method was demonstrated with a vehicle equipped with a laser scanner driving in urban environments. The method shows several potential benefits for a variety of methods that rely on a robust environment perception. Future work will focus on further improvement, quantitative evaluation and in using the method for navigation.

Acknowledgment

This work was partially funded by the German Federal Ministry of Economics and Technology through the research initiative UR:BAN (www.urban-online.org).

References

[1] A. Elfes, "Using occupancy grids for mobile robot perception and navigation," *Computer*, vol. 22, no. 6, pp. 46–57, Jun. 1989.

[2] C.-C. Wang and C. Thorpe, "Simultaneous localization and mapping with detection and tracking of moving objects," in *Proc. IEEE Int. Conf. Robotics and Automation*, vol. 3, 2002, pp. 2918–2924.

[3] T.-D. Vu, O. Aycard, and N. Appenrodt, "Online localization and mapping with moving object tracking in dynamic outdoor environments," in *IEEE Intelligent Vehicles Symp.*, 2007, pp. 190–195.

[4] C.-C. Wang, C. Thorpe, S. Thrun, M. Hebert, and H. Durrant-Whyte, "Simultaneous localization, mapping and moving object tracking," *Int. J. Robot. Res.*, vol. 26, no. 9, pp. 889–916, Sep. 2007.

[5] S. Pietzsch, T.-D. Vu, J. Burlet, O. Aycard, T. Hackbarth, N. Appenrodt, J. Dickmann, and B. Radig, "Results of a precrash application based on laser scanner and short-range radars," *IEEE Trans. Intell. Transp. Syst.*, vol. 10, no. 4, pp. 584–593, Dec. 2009.

[6] M. Bouzouraa and U. Hofmann, "Fusion of occupancy grid mapping and model based object tracking for driver assistance systems using laser and radar sensors," in *IEEE Intelligent Vehicles Symp.*, 2010, pp. 294–300.

[7] J. Moras, V. Cherfaoui, and P. Bonnifait, "Credibilist occupancy grids for vehicle perception in dynamic environments," in *Proc. IEEE Int. Conf. Robotics and Automation*, 2011, pp. 84–89.

[8] T.-N. Nguyen, B. Michaelis, A. Al-Hamadi, M. Tornow, and M. Meinecke, "Stereo-camera-based urban environment perception using occupancy grid and object tracking," *IEEE Trans. Intell. Transp. Syst.*, vol. 13, no. 1, pp. 154–165, Mar. 2012.

[9] G. Lidoris, D. Wollherr, and M. Buss, "Bayesian state estimation and behavior selection for autonomous robotic exploration in dynamic environments," in *Proc. IEEE/RSJ Int. Conf. Intelligent Robots and Systems*, 2008, pp. 1299–1306.

[10] C. Coué, C. Pradalier, C. Laugier, T. Fraichard, and P. Bessiere, "Bayesian occupancy filtering for multitarget tracking: an automotive application," *Int. J. Robot. Res.*, vol. 25, no. 1, pp. 19–30, Jan. 2006.

[11] M. Tay, K. Mekhnacha, C. Chen, M. Yguel, and C. Laugier, "An efficient formulation of the bayesian occupation filter for target tracking in dynamic environments," *Int. J. Veh. Auton. Syst.*, vol. 6, no. 1, pp. 155–171, Jan. 2008.

[12] T. Gindele, S. Brechtel, J. Schroder, and R. Dillmann, "Bayesian occupancy grid filter for dynamic environments using prior map knowledge," in *IEEE Intelligent Vehicles Symp.*, 2009, pp. 669–676.

[13] S. Brechtel, T. Gindele, and R. Dillmann, "Recursive importance sampling for efficient grid-based occupancy filtering in dynamic environments," in *Proc. IEEE Int. Conf. Robotics and Automation*, 2010, pp. 3932–3938.

[14] R. Danescu, F. Oniga, and S. Nedevschi, "Modeling and tracking the driving environment with a particle-based occupancy grid," *IEEE Trans. Intell. Transp. Syst.*, vol. 12, no. 4, pp. 1331–1342, Dec. 2011.

[15] S. Thrun, W. Burgard, and D. Fox, *Probabilistic Robotics (Intelligent Robotics and Autonomous Agents)*. The MIT Press, 2005.

[16] M. Montemerlo, S. Thrun, D. Koller, and B. Wegbreit, "FastSLAM: A factored solution to the simultaneous localization and mapping problem," in *Proc. AAAI Conf. Artificial Intelligence*, 2002, pp. 593–598.

[17] D. Pagac, E. Nebot, and H. Durrant-Whyte, "An evidential approach to map-building for autonomous vehicles," *IEEE Trans. Robot.*, vol. 14, no. 4, pp. 623–629, Aug. 1998.

[18] T. Yang and V. Aitken, "Evidential mapping for mobile robots with range sensors," *IEEE Trans. Instrum. Meas.*, vol. 55, no. 4, pp. 1422–1429, Aug. 2006.

[19] F. Homm, N. Kaempchen, J. Ota, and D. Burschka, "Efficient occupancy grid computation on the GPU with lidar and radar for road boundary detection," in *IEEE Intelligent Vehicles Symp.*, 2010, pp. 1006–1013.

[20] A. Jøsang and S. Pope, "Dempsters rule as seen by little colored balls," *Comput. Intell.*, vol. 28, no. 4, pp. 453–474, Nov. 2012.